2020 59th IEEE Conference on Decision and Control (CDC)
Jeju Island, Republic of Korea, December 14-18, 2020

On Time-Optimal Control of Elastic Joints under Input Constraints

Manuel Keppler[1] and Alessandro De Luca[2]

***Abstract*— We highlight the equivalence between the motion of an elastic joint and the two-body problem in classical mechanics. Based on this observation, a change of coordinates is introduced that reduces the two-body problem to a pair of decoupled one-body problems. This allows to treat the rest-to-rest motion problem with bounded actuator torque in an elegant geometric fashion. Instead of dealing directly with the fourth-order dynamics, we consider two equivalent masses whose motions have to be synchronized in separate phase spaces. Based on this idea, we derive a complete synthesis method for time-optimal rest-to-rest motions of this elastic system. The solution is a bang-bang control policy with one or three switches. We also introduce the concept of natural motions, when the minimum-time solution for the elastic and the rigid system is the same. The closed-form solutions obtained with our purely geometric approach verify the standard optimality conditions.**

I. Introduction

In recent years we have seen a surge in the application of robotic manipulators in new areas that require a dynamic interaction with the environment, e.g., shared work spaces with humans, healthcare, Industry 4.0. In order to facilitate these interactions in a safe manner, and to increase the mechanical robustness of robots against impacts, robot design evolved from rigid toward compliant actuators, i.e., soft robots. In addition, the inherent energy storing capabilities of such compliant actuators can be utilized for motion generation [1]. The intrinsic oscillatory dynamics can be exploited, for cyclic tasks such as locomotion, hammering, or drumming. For positioning tasks, however, these oscillatory dynamics require elaborate control concepts [2], [3] to achieve positioning performance that come close to that of rigid manipulators.

For many robotic applications, fast motion along a given path is crucial. It requires the exploitation of the maximal allowable actuator torques. Therefore, it is natural to aim at time-optimal solutions along a predefined path. The minimum-time optimization problem for rigid manipulators was treated first in [4], [5]. These methods rely on projecting the robot dynamics on the predefined trajectory. Using the parametric position and velocity along the path allows an elegant treatment of the problem in the phase plane. Unfortunately, these algorithms can not be applied to the presence of elastic joints. Other methods have been proposed to solve the time-optimal control problem for robots with (linear or nonlinear) flexible joints. In [6], a constrained optimal control problem is formulated to obtain an optimal motor trajectory. The problem of reaching a desired state in minimum time for visco-elastic joints under limited deflection has been treated in [7]. However, in order to simplify the analysis, these works contemplate a simplified model by considering the motors as ideal velocity sources. The time-optimal control problem for the complete elastic joint model was addressed also in [8], but only in a numerical way.

In this paper, we consider a system of two masses m and b connected by an elastic joint of stiffness k, as shown in Figure 1 (top). The corresponding dynamic model is

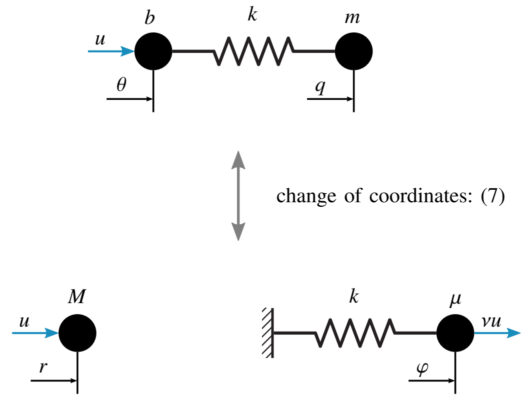

Fig. 1. The proposed change of coordinates reduces the two-body problem in eqs. (1–2) to a pair of one-body problems. With this transformation, the control input will act on both masses, although in a scaled fashion in one case.

$$m\ddot{q} + k(q - \theta) = 0 \tag{1}$$
$$b\ddot{\theta} + k(\theta - q) = u, \tag{2}$$

where θ and q are the positions of the two masses, relative to some inertial reference frame, and u is the control input force. We assume a symmetric bound on the input

$$|u| \leq \hat{u}. \tag{3}$$

We note that this model (with masses in translation) is equivalent to that of a robot joint (with rigid bodies in rotation), where the control torque u acts on the motor inertia b, driving the link inertia m through an elastic transmission of finite stiffness k. In this case, θ and q are the motor and link position, respectively.

For the elastic system (1–2), we present a method that simplifies generation and analysis of bang-bang control policies with bounded actuator torque. In contrast to previous works, rest-to-rest (RTR) solutions are obtained in closed form by means of geometric considerations only, providing thus valuable insight into the RTR motion problem. Further, no offline processing/optimization phase will be required.

We showcase the equivalence between the motion of the elastic system and the two-body problem in classical mechanics, introducing thus a change of coordinates that reduces the two-body problem to a pair of decoupled one-body problems. In contrast to a two-body problem in classical mechanics, additional external forces are exerted on each mass. These forces are directly related to our control input. This approach allows to extend the idea of phase-plane based optimization [4], [5] to the presence of elastic joints. However, instead of working with the projected dynamics in a single phase-space diagram, we face the problem of synchronizing the motion of two bodies in two separate phase planes. In this framework, we derive conditions under which the elastic joint system achieves time-optimal motion in the rest-to-rest (RTR) problem in a total time equal to that of a rigid joint (i.e., for $k \to \infty$). Thus, an elastic joint system

[1]Institute of Robotics and Mechatronics, German Aerospace Center (DLR), 82234 Oberpfaffenhofen, Germany. manuel.keppler@dlr.de
[2]Dipartimento di Ingegneria Informatica, Automatica e Gestionale, Sapienza Università di Roma, Italy. deluca@diag.uniroma1.it

978-1-7281-7446-4/20/$31.00 ©2020 IEEE

matches the performance of a rigid one only for these special cases that we define as natural motions. As a result, our analysis may be used also to optimize the mechanical design of an elastic transmission.

The rest of the paper is organized as follows. In Section II, we introduce the change of coordinates that decouples the dynamics of the elastic joint system. Section III presents the concept of natural motions, and the associated bang-bang solution with a single control switch to the minimum time problem. In Section IV, we generalize the solution to a generic RTR motion, synthesizing the time-optimal bang-bang policy with three control switchings. Numerical results are reported in Section V.

II. Equivalence Transformation

In classical mechanics, the two-body problem predicts the motion of two masses, each exerting a force on the other. One of the prominent examples is the gravitational case, also known as Kepler problem [9], [10], which arises in orbital mechanics for predicting the orbits of two bodies in a binary system[1]. This problem can be treated in an elegant fashion by reducing it to a pair of one-body problems. Substituting Newton's law of universal gravitation [11] with Hooke's law, we can treat the elastic joint system (1–2) as a two-body problem that evolves in one dimension, allowing to apply the techniques that simplified the analysis of the Kepler problem.

In our elastic system, each body exerts a conservative central force on the other (Figure 1). In addition, one of the two bodies is subject to an external force which represents our control input. The force of interaction is the elastic force $k(\theta - q)$. This suggests that we may conveniently use the relative position as one of the generalized coordinates

$$\varphi \triangleq \theta - q, \tag{4}$$

letting the potential energy of the system take the simple form

$$\mathcal{V} = \tfrac{1}{2}k\,(\theta - q)^2 = \tfrac{1}{2}k\varphi^2. \tag{5}$$

A good choice for the second generalized coordinate turns out to be the position of the center of mass (CoM) of the system

$$r \triangleq \frac{mq + b\theta}{M}, \tag{6}$$

where $M \triangleq m + b$ is the total mass of the two bodies. The original set of coordinates is related to the introduced one by the inverse transformation

$$q = r - \frac{b}{M}\varphi; \quad \theta = r + \frac{m}{M}\varphi. \tag{7}$$

Thus, we can rewrite the kinetic energy of the system as

$$\mathcal{T} = \tfrac{1}{2}\left(m\dot{q}^2 + b\dot{\theta}^2\right) = \tfrac{1}{2}\left(M\dot{r}^2 + \mu\dot{\varphi}^2\right), \tag{8}$$

with the *reduced mass* $\mu \triangleq \frac{mb}{m+b} < \min(m, b)$. The kinetic energy of the system is thus equal to that of two virtual particles, one of total mass M moving with the speed of the CoM, and the other of reduced mass μ moving with the speed of the relative position. The total energy of the system,

$$\mathcal{H} = \tfrac{1}{2}M\dot{r}^2 + \tfrac{1}{2}\left(\mu\dot{\varphi}^2 + k\varphi^2\right) \triangleq \mathcal{H}_{\text{com}} + \mathcal{H}_{\text{rel}}, \tag{9}$$

shows the decoupled nature of the two one-body problems. This structure significantly simplifies matters. The equations of motion in the new coordinates are in fact

$$M\ddot{r} = u \tag{10}$$

$$\mu\ddot{\varphi} + k\varphi = \nu u, \tag{11}$$

with the dimensionless parameter $\nu \triangleq m/M$. As predicted (see also the bottom of Figure 1), equation (10) is precisely that of a free floating particle of mass M driven by u, while (11) represents a mass μ oscillating about a fixed center while subject to the external force u scaled by the constant factor ν. We note also that, given a constant input, the elastic joint system is invariant to time reversal, i.e., under the operation $T : t \mapsto -t$. Intuitively speaking, this is due to the conservation of entropy. This property will turn out to be extremely useful later in the paper.

A. Solution of the Decoupled Systems

Since we are interested in bang-bang control policies, we assume that u is piece-wise constant. In this case, the solution to the equation of motion (10) is trivial

$$r(t) = \frac{u}{2M}t^2 + C_1 t + C_2, \tag{12}$$

with C_1 being the initial velocity and C_2 being the initial position. Since we are interested in RTR motions we can assume, without loss of generality[2], that $C_1 = 0$ and $C_2 = 0$. The general solution of (11) is

$$\varphi(t) = A\cos(\omega t + \delta) + \bar{u}, \tag{13}$$

with oscillation amplitude A, *angular frequency* $\omega \triangleq \sqrt{k/\mu}$, phase shift δ, and *static response*

$$\bar{u} \triangleq \nu u/k. \tag{14}$$

The amplitude and phase shift depend on the initial conditions. The corresponding velocity is given by

$$\dot{\varphi}(t) = -A\omega\sin(\omega t + \delta). \tag{15}$$

We can represent the phase space trajectory of system (11) in a useful way by moving into the complex plane. To this end, we express (13) and (15) in terms of complex exponentials. The system state will be a single point in the complex plane, i.e., the complex plane serves as phase plane. To this end, let

$$z(t) \triangleq \bar{u} + \varphi(t) + i\dot{\varphi}(t) = \bar{u} + A_1 e^{i(\omega t + \delta)} + A_2 e^{-i(\omega t + \delta)}, \tag{16}$$

with $A_1 \triangleq \frac{A}{2}(1 - \omega)$ and $A_2 \triangleq \frac{A}{2}(1 + \omega)$. As the reduced mass oscillates back and forth, point z moves on an ellipse centered at $\bar{u}$ in clockwise orientation. This result is illustrated in Figure 2. The exact shape will become clear in a moment.

Observe that the state trajectory becomes particularly simple for $\omega = 1$, when the ellipse in the phase plane degenerates to a circle. Exploiting this fact to simplify matters, we rewrite (13)–(15) in terms of the scaled time

$$\tau = \omega t, \tag{17}$$

that we shall refer to as *natural time* (which is system specific, as the scaling factor is its angular frequency). Using the chain rule $d(\cdot)/dt = \omega\, d(\cdot)/d\tau$, we have

$$\varphi(t) = \varphi(\tau/\omega), \tag{18a}$$

$$\dot{\varphi}(t) = \omega\varphi'(\tau/\omega), \tag{18b}$$

[1]In the simplest case, each of the two bodies exert a conservative, central force on the other, with no other external force being present.

[2]We can always choose the inertial frame so that $r(t)|_{t=0} = 0$.

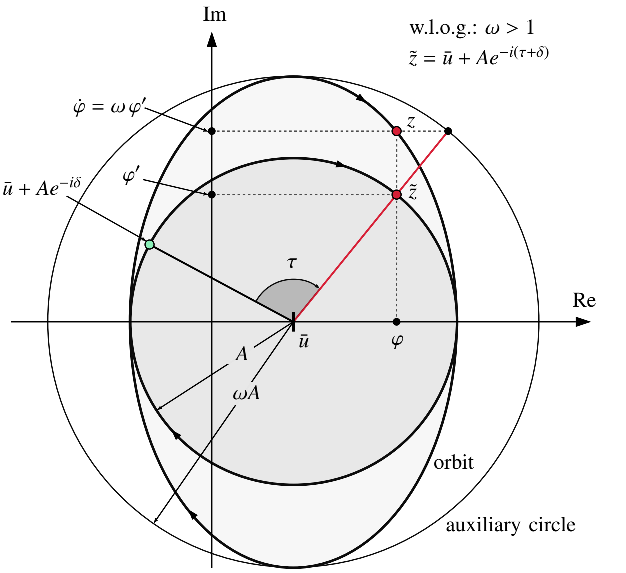

Fig. 2. The position $(\varphi, i\varphi')$ of the normalized system is given by the complex pointer $Ae^{i(\tau+\delta)}$ whose origin is offset along the real axis by $\bar{u}$. As the reduced mass oscillates back and forth, this point moves in clockwise orientation on an inscribed circle with radius A that is centered at $\bar{u}$. The elliptic orbit of the reduced mass $(\varphi, \dot{\varphi})$ can be obtained by scaling the imaginary part of $\tilde{z}$, i. e. φ', by ω.

with the natural time as parameter, and having denoted by $(\cdot)' \triangleq d(\cdot)/d\tau$ the new differential operator. We note that (φ, φ') are equivalent to the analytical solution of a clamped spring-mass system with natural frequency $\omega = 1$. The scaled trajectory

$$\tilde{z}(\tau) = \bar{u} + \varphi(\tau) + i\varphi'(\tau) = \bar{u} + Ae^{i(\tau+\delta)}, \tag{19}$$

corresponds then to the solution of a spring-mass system with a unitary angular frequency. Thus, a phase plane trajectory z can be obtained from the trajectory $\tilde{z}$ by scaling the imaginary part of $\tilde{z}$ by the constant factor ω.

If we know the trajectory $\tilde{z}(\tau/\omega)$ in the complex plane, we obtain $z(t)$ by stretching ($\omega > 1$) or squeezing ($\omega < 1$) the imaginary part of $\tilde{z}$ by the angular frequency factor. It is straightforward to see that $\tilde{z}$ defines a point that moves in the clockwise direction on a circle centered at $\bar{u}$ and having radius A. Hence, z will trace an ellipse centered at $\bar{u}$, with axes parallel to the coordinate axes, semi-major axis ($\omega > 1$) of length ωA and semi-minor axis of length A.

Note finally that the natural time τ, with δ as an offset, corresponds to the polar angular coordinate of $\tilde{z}$, but not to the polar angular coordinate of z. However, the parameter pair τ and δ can be interpreted as the eccentric anomaly [12] of a point z that moves on an elliptic orbit, a popular concept in astronomy. The geometric meaning of the eccentric anomaly becomes clear in the point construction method of an ellipse by La Hire. Given a trajectory $\tilde{z}(\tau/\omega)$, this construction method allows to derive the corresponding trajectory $z(t)$, and vice versa, in a purely geometric way, see Figure 2.

III. Natural Motions

We preliminarily recap the rest-to-rest motion in minimum time of the total mass M made by the two individual masses m and b connected by a rigid joint ($k \to \infty$). We transfer then these insights to the case of an elastic joint and introduce the concept of *natural motions*. When a natural motion applies, this associated rest-to-rest command is time optimal. Further, natural motions are the only cases when an elastic joint matches the fastest RTR motion performance of a rigid joint.

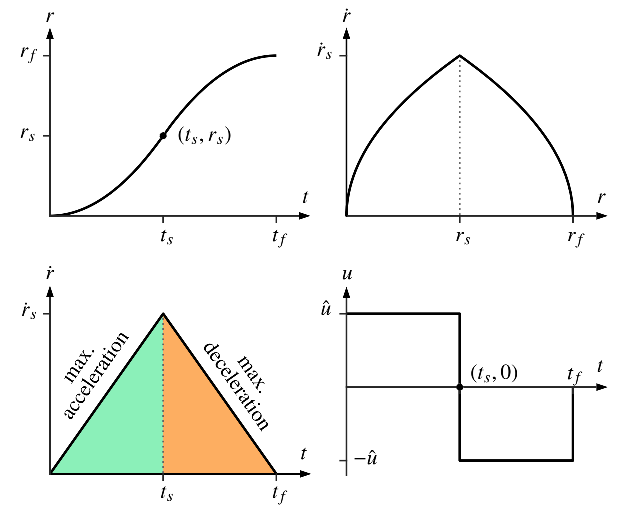

Fig. 3. A typical time-optimal RTR motion profile for a rigid joint. We have points and lines of symmetry. The total area under the velocity profile is equal to the total displacement $r_f > 0$. The CoM trajectory of an elastic joint has the same form for the natural motion case.

A. Rigid Joint Case

Consider (10) as the dynamics of the rigid joint case. The minimum time control problem to displace by a desired amount r_f the total mass M from rest to rest, under the constraint (3), reduces to a minimum time problem for a double integrator with constant bounds on the acceleration input $\ddot{r}$. From (3), the upper and lower bounds for the acceleration are $\ddot{r}_{\max} = \hat{u}/M$ and $\ddot{r}_{\min} = -\hat{u}/M$. Throughout this paper we assume, w.l.o.g, that $r_f > 0$.[3] The solution to the optimal control problem is a bang-bang input [13]. Due to the symmetry of the constraints (3) and the time symmetry of (10) under constant inputs, the solution will also be symmetric with respect to time and has the form

$$\ddot{r} = \begin{cases} \ddot{r}_{\max}, & \text{for } 0 \le t \le t_s \\ \ddot{r}_{\min}, & \text{for } t_s < t \le t_f, \end{cases} \tag{20}$$

where t_f denotes the final time and $t_s \triangleq t_f/2$ the instant of command switching. Obviously, this corresponds to the control law

$$u = \begin{cases} \hat{u}, & \text{for } 0 \le t \le t_s \\ -\hat{u}, & \text{for } t_s < t \le t_f, \end{cases} \tag{21}$$

which yields the system response

$$r(t) = \begin{cases} \frac{\hat{u}}{2M} t^2, & \text{for } 0 \ge t \ge t_s \\ -\frac{\hat{u}}{2M}(t^2 - 4t_s t + 2t_s^2), & \text{for } t_s < t \ge t_f \end{cases} \tag{22}$$

and

$$\dot{r}(t) = \begin{cases} \frac{\hat{u}}{M} t, & \text{for } 0 \ge t \ge t_s \\ -\frac{\hat{u}}{M}(t - 2t_s), & \text{for } t_s < t \ge t_f. \end{cases} \tag{23}$$

The response to a bang-bang input (21) is shown in Figure 3.

B. Elastic Joint Case

We know that the class of bang-bang inputs (21) solve the time-optimal control problem in the rigid joint case. We are interested in whether such solutions exist and are optimal also for the elastic case, when the task is to move

[3]The solutions for $r_f < 0$ are simply obtained by inverting the input signs.

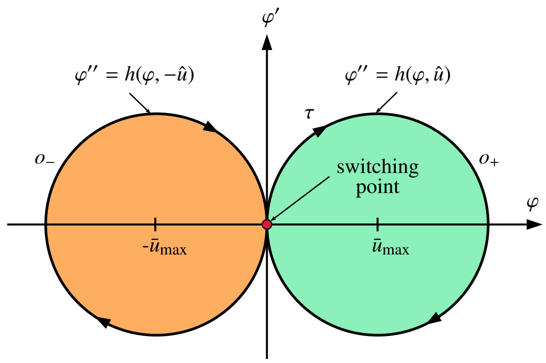

Fig. 4. A natural motion trajectory of the reduced mass with one switching event. The orbit o_+ (o_-) is the locus of all points (φ, φ') which can be transferred to the origin by the control $u = \hat{u}$ ($u = -\hat{u}$).

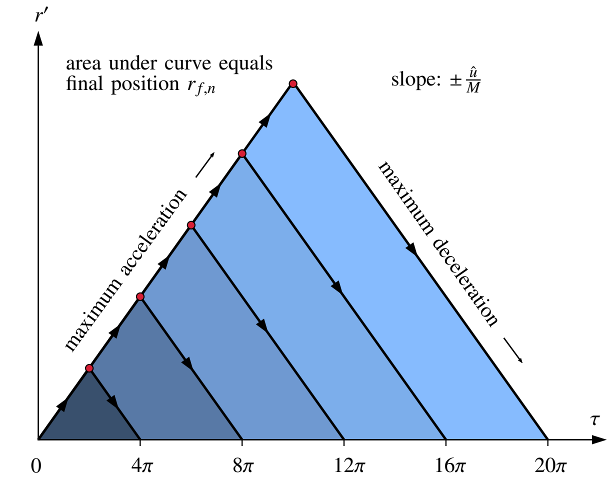

Fig. 5. Typical natural motion velocity profiles for the CoM. The red dots indicate the switching events for $n = 1, 2, \ldots$ full acceleration/deceleration cycles. This construction process can be continued ad infinum by adding further acceleration and deceleration orbits.

the entire system (10)–(11) from rest to rest, with initial and final positions

$$r(t) = \begin{cases} 0, & \text{for } t = 0 \\ r_f > 0, & \text{for } t = t_f \end{cases}, \quad \varphi(t) = \begin{cases} 0, & \text{for } t = 0 \\ 0, & \text{for } t = t_f. \end{cases} \tag{24}$$

The result for the rigid case allows to conclude that a bang-bang input yields the time-optimal rest-to-rest motion for the CoM of the flexible joint system. The solution is equivalent to the one show in Figure 3. However, since we are interested in moving the entire system from rest to rest (and with zero final deformation), we have to ensure that our control input induces a synchronized motion for the CoM and the reduced mass μ. The acceleration of the reduced mass subject to the bang-bang input (21) is

$$\ddot{\varphi}(t) = \omega^2 \varphi''(\tau/\omega) = \begin{cases} f(\varphi, \hat{u}), & \text{for } 0 \le t \le t_s \\ f(\varphi, -\hat{u}), & \text{for } t_s \le t \le t_f \end{cases} \tag{25}$$

where $f(\varphi, u) \triangleq \mu^{-1}(\nu u - k\varphi)$. In order to simplify the notation, let $h(\varphi, u) \triangleq \omega^{-2} f(\varphi, u)$ such that $\varphi''(\tau/\omega) = h(\varphi, u)$. Also, denote for compactness $\bar{u}_{\max} \triangleq \nu\hat{u}/k$.

As we prove below, there exist indeed bang-bang inputs of the form (21) that yield synchronized RTR motions satisfying the boundary conditions (24). The most intuitive approach to find the switching position is to build the switching curve in the $(\varphi, i\varphi')$ phase plane. We start with maximum acceleration and solve $\varphi'' = f(\varphi, \hat{u})$ forward in time from the initial point $\varphi = \varphi' = 0$. From (19), we know that for a constant input u all solutions are circles centered at $\bar{u}$ which are traced in the clockwise direction. As such, a system that starts from the origin, under $u = \hat{u}$, moves clockwise on the orbit o_+ with radius $A = \bar{u}_{\max}$. This behavior is shown in Figure 4, as well as on the left in Figure 6 (where the natural time τ corresponds to the blue angle that is being covered).

Next, we solve $\varphi'' = f(\varphi, -\hat{u})$ backward in time from the final point $\varphi = \varphi' = 0$, yielding the circular orbit o_-. Since system (10–11) under a constant input is invariant to time reversal, forward and backward integration are equivalent operations when starting from a given system state. Therefore, we don't need to solve the system dynamics backwards in time: due to the control policy (21), forward and backward trajectories are just mirror images with respect to the imaginary axis.

We note also that the two trajectories are tangent at the origin of the phase plane. Since no other point of tangency or intersection exists, transfer between the two orbits may occur only at the origin. The phase plane trajectory that emerges from solving $\varphi'' = h(\varphi, -\hat{u})$ backwards in time from $\varphi = \varphi' = 0$ is the switching curve for this scenario. The optimal control policy is to apply maximum acceleration $\varphi'' = h(\varphi, \hat{u})$ until the trajectory intersects the origin, and then switch to maximum deceleration $\varphi'' = h(\varphi, -\hat{u})$.

The acceleration and deceleration phases are in the time intervals $0 < \tau \le 2\pi$ and $2\pi < \tau \le 4\pi$, respectively. Hence, we spend half of the time applying $u = \hat{u}$ and the remaining half applying $u = -\hat{u}$. Since this strategy is time optimal for the RTR motion of the CoM, we conclude that this control policy moves the entire system (10)–(11) from rest to rest in a time-optimal way[4].

We can immediately see that there exists an infinite number of such solutions. In fact, we may cover n orbits with maximum acceleration and n orbits with maximum deceleration. We refer to all these instances as natural motions. All natural RTR motions of system (1–2) emerge from the control policy

$$u = \begin{cases} \hat{u}, & \text{for } 0 \le \tau \le \tau_{s,n} \\ -\hat{u}, & \text{for } \tau_{s,n} < \tau \le \tau_{f,n}. \end{cases} \tag{26}$$

with $\tau_{f,n} = 4n\pi$ and $\tau_{s,n} = \tau_{f,n}/2$, for $n \in \mathbb{N}$. Furthermore, each natural motion is a time-optimal solution to a specific RTR motion problem for the elastic joint system.

The velocity profile of the CoM mass subject to the control (26) is piece-wise linear, as shown in Figure 5. The geometric relation between the CoM velocity r' and the corresponding final positions r_f is given by

$$r_f = \int_0^{t_f} \dot{r}\, dt = \int_0^{\tau_f} r'\, d\tau. \tag{27}$$

Thus, the final position $r_{f,n}$ is equal to the area under the corresponding velocity profile in Figure 5. From (23), we know that the peak velocity at the switching point n is given by $\dot{r}(t_{s,n}) = (\hat{u}/M)(\tau_{s,n}/\omega)$. Applying basic geometry allows to determine the final reached position as[5]

$$r_{f,n} = \frac{\hat{u}}{M}\left(\frac{\tau_{s,n}}{\omega}\right)^2 = \frac{\hat{u}}{M}\left(\frac{2n\pi}{\omega}\right)^2. \tag{28}$$

[4] Recall that we have two decoupled systems. As such, the minimum possible time for moving both systems synchronously has to be greater or equal to the minimum times for moving the individual systems.

[5] Note that we cover half of the distance in half of the time.

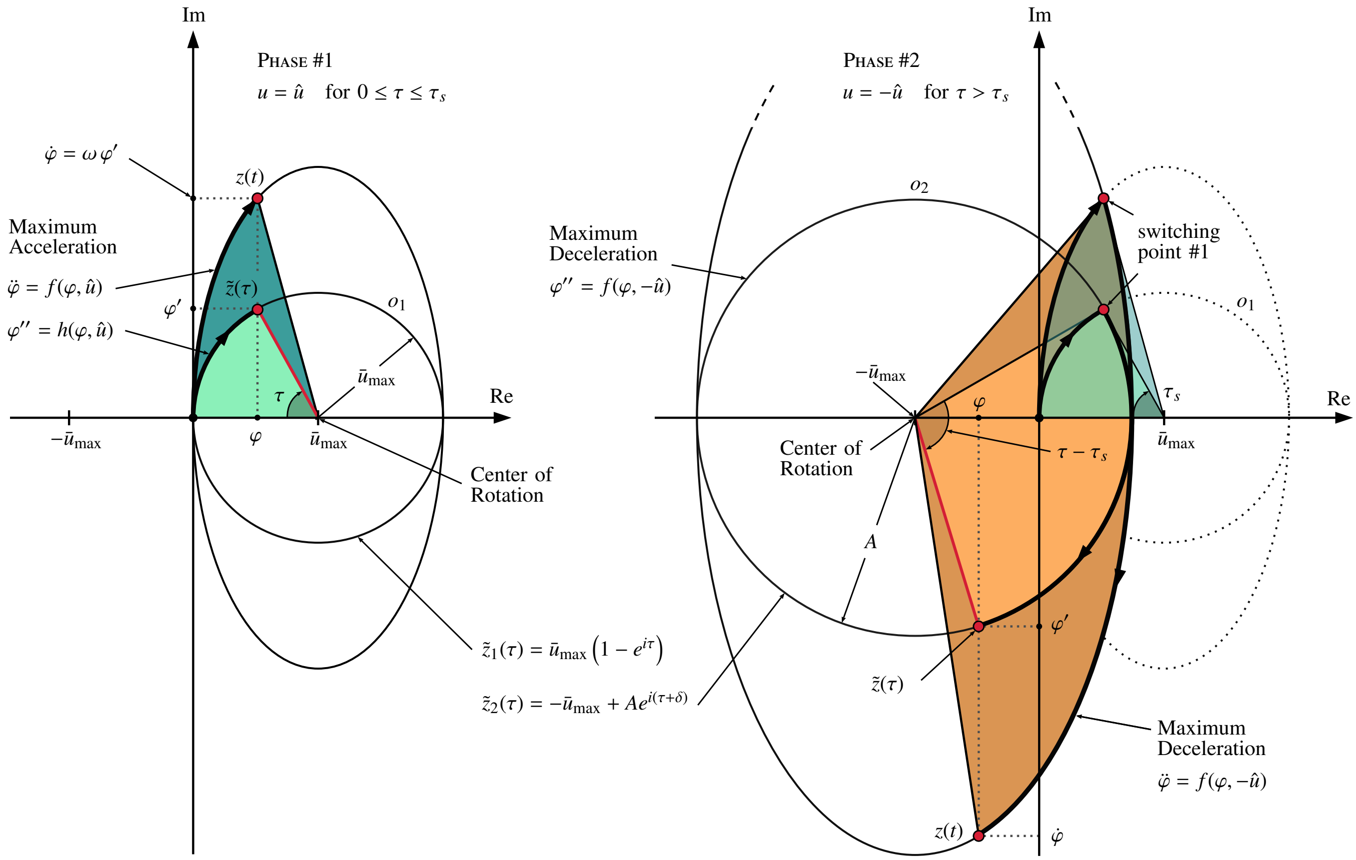

Fig. 6. Geometry of the phase-space trajectories for multiple switching incidents.

Indeed, the achievable final positions are countable and do not cover the entire set $\mathbb{R}^+$. We may only reach (infinitely many) discrete points for a given set of system parameters. In the following section, we present the class of bang-bang solutions that allows to cover the entire set of real numbers.

IV. Reaching any Distance

In this section, we synthesize a three-switching bang-bang control strategy that achieves RTR motions in minimum time for arbitrary final positions .

A. The Synchronization Problem

By introducing three switching points, we will show that one can reach any desired position for the CoM as well. Again, we synchronize the motion of the CoM with the motion of the reduced mass so that the boundary conditions (24) are all satisfied. From the time-symmetry of the dynamics, we observe that any time-optimal control strategy must be symmetric with respect to the half motion time. Thus, we only consider three-switching strategies that satisfy this condition. Therefore, a policy including three control switches (for $r_f > 0$) must be of the form

$$u = \begin{cases} \hat{u}, & \text{for } 0 \le \tau \le \alpha_1 \\ -\hat{u}, & \text{for } \alpha_1 < \tau \le \alpha_1 + \alpha_2 \\ \hat{u}, & \text{for } \alpha_1 + \alpha_2 < \tau \le \alpha_1 + 2\alpha_2 \\ -\hat{u}, & \text{for } \alpha_1 + 2\alpha_2 < \tau \le 2\left(\alpha_1 + \alpha_2\right). \end{cases} \tag{29}$$

When applying an input torque $\hat{u}$ to system (10)–(11), and starting from the origin, we know that the resulting trajectory

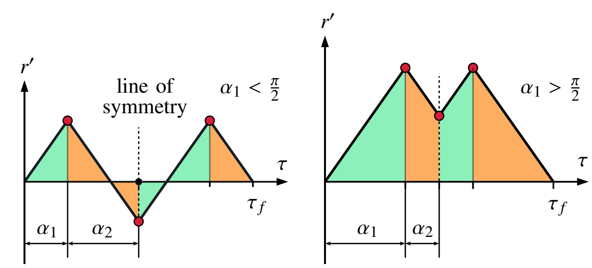

Fig. 7. Typical CoM velocity profiles for the three-switchings solution. By purely geometrical reasoning we may conclude that the CoM velocity assumes negative values if and only if $\alpha_1 < \pi/2$.

for $\tilde{z}$ is a circular orbit o_1 centered at $\bar{u}_{\max}$ —see the left side of Figure 6. Switching to an input $-\hat{u}$ after some time $\tau_{s1,n}$ transfers $\tilde{z}$ to a circular orbit o_2 with its center at $-\bar{u}_{\max}$. The continuity of the solution (φ, φ') implies that these two circular orbits intersect at the switching time τ_s. This uniquely defines the radius of orbit o_2. At the time-point of switching, the amplitude A in (19) assumes the radius of o_2. In a switching event, we can think of an amplitude A and angular offset δ adaptation such that continuity of the solution for (φ, φ') is ensured. This construction is illustrated on the right side of Figure 6. We remark that a continuous solution in (φ, φ') imply a continuous solution in $(\varphi, \dot{\varphi})$. Also, since we require the CoM to complete the motion at rest, the total intervals of maximum acceleration and of maximum deceleration must be equal. This is visualized in Figure 7.

We are now in the position to derive a control policy with

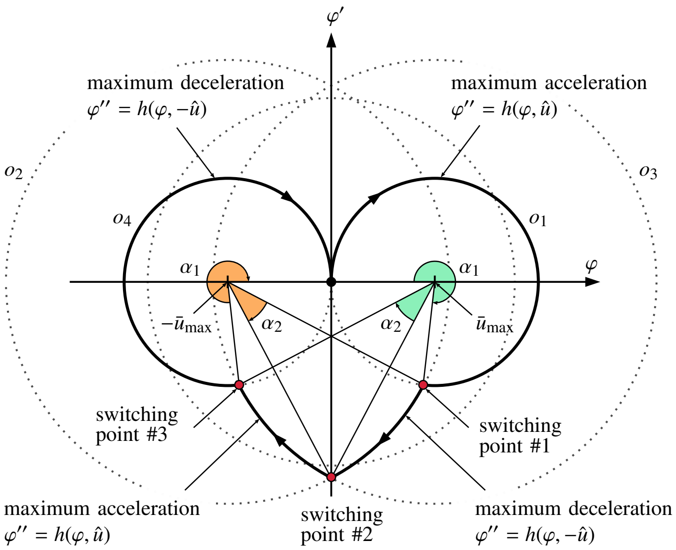

Fig. 8. A symmetric three-switchings trajectory for the reduced mass. Note that it is possible to cover the maximum acceleration orbit o_1 multiple times before transferring to orbit o_2. However, symmetry demands that for n maximum acceleration cycles on orbit o_1 we enter n maximum deceleration cycles on orbit o_4.

three switches that allows us to achieve any final rest position for the CoM, while simultaneously moving the reduced mass from rest to rest. We shall build the phase plane trajectory of the reduced mass that correspond to a three-switching control policy, as shown in Figure 7. A typical trajectory of this type is shown in Figure 8.

The first two phases of maximum and minimum acceleration yield orbit o_1 and the transfer to orbit o_2. The time spent on orbit o_1 corresponds to the polar angle α_1. The actual time span is related to the scaled one by the relation $t = \omega^{-1}\tau$. In a similar way, the polar angle α_2 corresponds to the time spent on the deceleration orbit o_2. Imagine now to perform the same procedure of trajectory construction backward in time. We know that our final position shall be the origin. Thus, we start by integrating $\varphi'' = f(\varphi, -\hat{u})$ backward in time from the origin of the phase plane, which yields orbit o_4. After some time α_1, we switch to full acceleration and obtain orbit o_3. We observe that by choosing α_1 and then α_2 wisely, we will have the second command switching exactly where the orbits o_2 and o_3 intersect for the first time. Recall now that forward and backward integration for our system are equivalent operations. Thus, the forward and backward trajectories, due to the above control policy, must be mirror images with respect to the imaginary axis. This implies that the switching must happen where the phase plane trajectory intersects the imaginary axis (i.e., when $\varphi = 0$).

We conclude that this geometric construction yields cyclic trajectories for the reduced mass, moving it from rest to rest. Further, due to our assumptions above, the same control policy yields also rest-to-rest motions for the CoM. We show next that we can reach any distance (in particular, between two natural motions) by adjusting the value of α_1.

B. Solution by Phase Space Geometry

Let us start with some geometric observations. Clearly, the radius of the first orbit o_1 is $R_1 = \bar{u}_{\max}$. The relation between the first switching angle α_1 and the radius of the second orbit o_2, as shown in Figure 9, is given by

$$R_2 = \bar{u}_{\max} \sqrt{5 - 4\cos(\alpha_1)}. \tag{30}$$

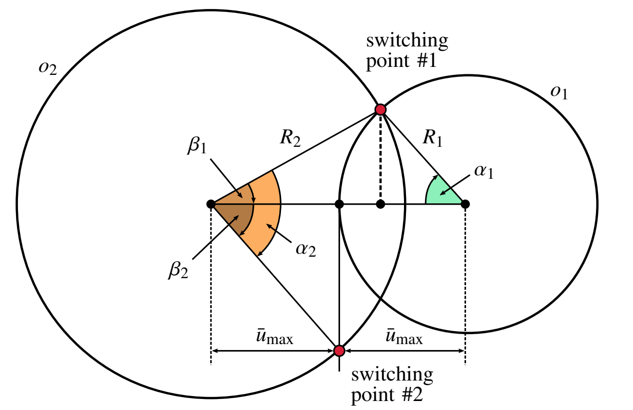

Fig. 9. Geometric derivation of the dependence of α_2 on α_1.

We simplify the derivation of the angle α_2 by introducing two intermediary angles β_1 and β_2, which are defined in Figure 9. For these two angles we can derive the following relations

$$\beta_1 = \arcsin\left(\frac{R_1}{R_2}\sin(\alpha_1)\right) = \arcsin\left(\frac{\sin(\alpha_1)}{\sqrt{5 - 4\cos(\alpha_1)}}\right)$$

$$\beta_2 = \arccos\left(\frac{\hat{u}}{R_2}\right) = \arccos\left(\frac{1}{\sqrt{5 - 4\cos(\alpha_1)}}\right).$$

Note that both intermediary angles are solely a function of the first switching time point α_1. In turn, this implies that α_2 is a function of α_1. We have

$$\alpha_2 = \beta_1 + \beta_2, \tag{31}$$

which is zero if and only if $\alpha_1 = 2\pi n$, as expected. Recall that the final position is given by (27). The integral corresponds to the area under the curves in Figure 7 on the right. This area can be derived through purely geometric reasoning, and is equal to

$$r_f(\alpha_1) = \frac{\hat{u}}{M\omega^2}\left(2\alpha_1^2 - (\alpha_1 - \alpha_2)^2\right). \tag{32}$$

The corresponding natural time required to reach $r_f > 0$ is

$$\tau_f(\alpha_1) = 2\,(\alpha_1 + \alpha_2)\,. \tag{33}$$

Is it easy to verify that, for the degenerate case of $\alpha_2 = 0$, we obtain just one of the natural motion solutions (28).

Finally, Figure 10 shows the mapping between the final (natural) motion time τ_f and the desired motion displacement $r_f > 0$, as a result of relations (31) to (33). One can immediately see that, for all but the natural motion cases, the minimum time needed for a RTR motion realizing a desired displacement r_f of the CoM is always larger in the flexible case in comparison to the rigid case. Anyway, differences tend to vanish for longer displacements (as well as for increasing values of the joint stiffness k).

C. Optimality Result

We conclude this section with the following proposition.

Proposition 1. *Given the initial and desired final positions of the form (24) for system (1–2), the three-switching bang-bang control policy (29) provides the time-optimal solution for rest-to-rest motions. If the final position satisfies condition (28), the control policy (29) degenerates to a single switching bang-bang input which results in a natural motion.*

We sketch here the verification of the time-optimality of the three-switching strategy, based on a procedure that uses

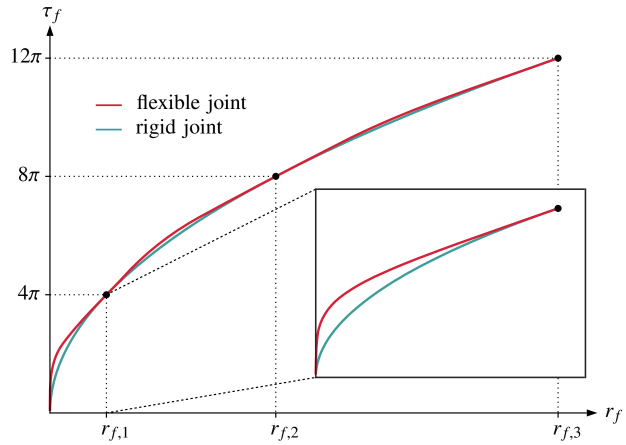

Fig. 10. A comparison of the three-switching control policy, including natural motion solutions, versus the time-optimal RTR solutions for a rigid joint. Note, the natural motion solutions of a flexible joint match the time-optimal solutions for a rigid joint. Otherwise, a flexible joint is always inferior for RTR motions. However, for motions that take longer than 4π this mismatch, in relation to the total time τ_f, becomes negligible.

Pontryagin's minimum principle [13]. For our linear, single-input, time-invariant, and controllable system, we deal with a *normal* time-optimal problem, and therefore singular arcs in the optimal solution can be ruled out. Pontryagin's minimum principle provides then the optimal control as a piece-wise constant function of time, which is always in saturation (i.e., bang-bang) except in isolated instants of switching. The sign of the control law $u^*(t)$ is determined by the sign of the switching function $s(t)$, which in our case depends on the evolution of two components of the optimal costate vector $\boldsymbol{\lambda}(t) \in \mathbb{R}^4$. We impose then equality to zero of the Hamiltonian $\mathcal{H}(t)$ at the initial and final times, $t = 0$ and $t = t_f$, using the known boundary conditions of the problem, the optimal values of our control profile, $u^*(0)$ and $u^*(t_f)$, and the final time t_f obtained from our geometric approach. Similarly, we impose in two out of the three instants of control switching, namely $t_1 = \alpha_1/\omega$ and $t_2 = t_f/2$ (both obtained from our geometric computations), the vanishing of the switching function, $s(t_1) = s(t_2) = 0$. In this way, we set up a well-defined linear system of equations that allows us to determine the four initial costate values, i.e., $\lambda_i(0)$, $i = 1, \ldots, 4$. With these, we integrate forward the necessary conditions of optimality and obtain analytically the unique expression of the optimal costate $\boldsymbol{\lambda}^*(t)$ and of the associated switching function $s^*(t)$. We verify then that the crossing of zero of this function occurs only at the switching instants of our control policy and that the sign of $s^*(t)$ elsewhere is always opposite to the sign of our $u^*(t)$. Moreover, using forward integration of the state equations driven by our optimal control, we obtained also the optimal state evolution $\boldsymbol{x}^*(t)$. With all these values plugged into the Hamiltonian, we finally verify that $\mathcal{H}(t) = 0$ at any time $t \in [0, t_f]$. Therefore, our solution satisfies the minimum principle of Pontryagin and the necessary conditions of optimality.

V. Numerical results

As reference motions, we have considered the three examples presented by Dahl in [8]. The parameters of the considered two-mass system are $m = b = 0.5$ [kg], whereas the bound on the input force is $\hat{u} = 1$ [N]. The results are summarized in Table I. We refer to the three sets of system parameters (for different values of the stiffness k) as Case 1 to Case 3.

TABLE I

k [N/m]	ω [rad/s]	α_1 [rad]	α_2 [rad]	r_f [m]	τ_f [rad]	t_f [s]
1	2	2.032	1.528	2	2.27π	3.56
10	6.325	7.653	1.558	2	5.86π	2.91
100	20	26.803	1.567	2	18.08π	2.84

Our geometric control policy (29) yields exactly the same solutions presented by [8]. It important to remark that those optimal solutions were obtained through numerical optimization. In contrast, we provide a closed-form solution to the problem.

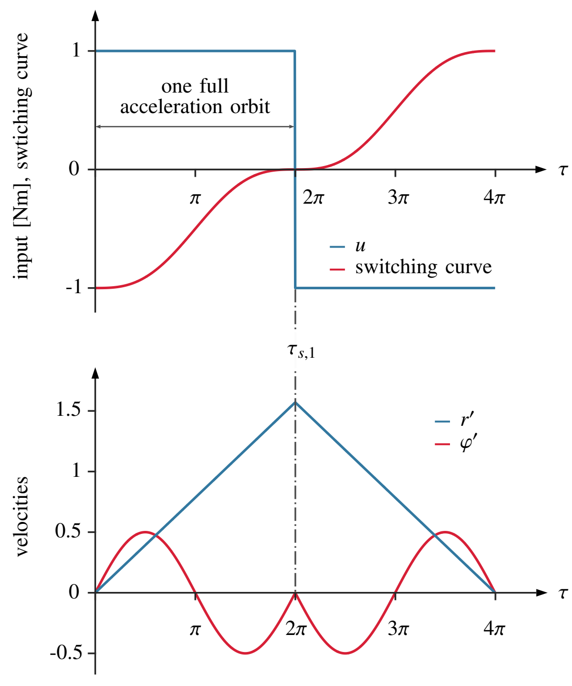

Fig. 11. The first natural motion for Case 1: $r_f = \pi^2$ m, $\tau_f = 4\pi$ rad.

In Figure 11, we show the time-optimal bang-bang control for the first natural motion in Case 1 ($k = 1\ \mathrm{N\,m^{-1}}$). The final position, as given by (28) with $n = 1$, is $r_f = \pi^2$. In the top part, we have plotted also the optimal switching function.

Figure 12 shows the time-optimal control law with three switchings, the optimal switching function, and the two state velocities that result from control policy (29) in Case 2 ($k = 10\ \mathrm{N\,m^{-1}}$). The zero crossings of the switching function match the switching instants of our control policy (29). This confirms the conclusion about the achieved time-optimality with our geometric approach.

VI. Conclusion

In this paper we highlighted the connection between a two-mass system with an elastic joint and the two-body problem in classical mechanics. Based on this insight, we introduced a change of coordinates that decouples the complete dynamics into a pair of single-body problems. This simplification allowed us to apply pure geometrical reasoning to generate and analyse minimum-time bang-bang solutions to the rest-to-rest (RTR) motion problem under actuator torque bounds. All solutions are provided in closed form. Further, we introduced the concept of natural motions which are time-optimal solutions to the RTR motion problem. These are the

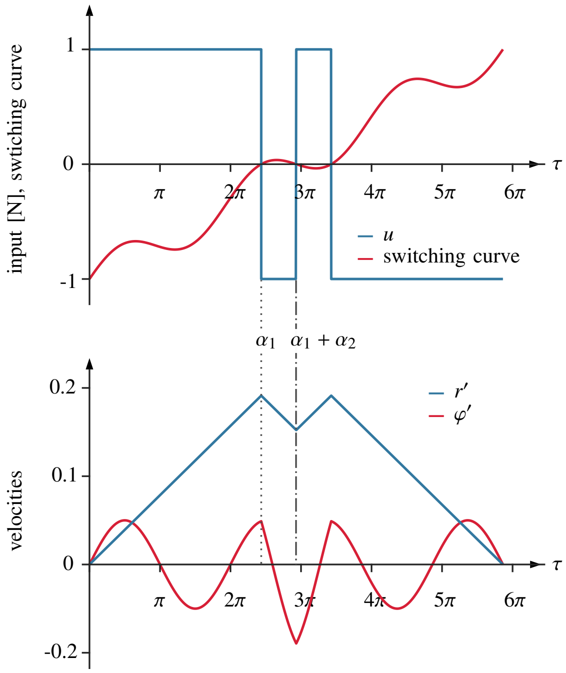

Fig. 12. Three-switchings solution for Case 2: $r_f = 2$ m, $\tau_f = 5.86\pi$ rad.

only RTR solutions where the minimum-time performance of an elastic joint system matches that of a rigid joint.

The insight obtained from the natural motion analysis, can be exploited to optimize the design of an elastic robot joint. In fact, it is desirable that the natural motion of an elastic joint matches its nominal motion. Only in this case, the RTR motion in the elastic case can reach the motion time performance of a rigid joint. Our framework can be easily extended to account for limitations on joint deflections and motor velocities. The natural motion concept could be extended to include periodic motions, like in pick-and-place robotic tasks. These issues will be the subject of future investigations.

References

[1] D. Braun, M. Howard, and S. Vijayakumar, "Optimal variable stiffness control: Formulation and application to explosive movement tasks," *Autonomous Robots*, vol. 33, no. 3, pp. 238–253, 2012.

[2] M. Keppler, D. Lakatos, C. Ott, and A. Albu-Schäffer, "Elastic structure preserving (ESP) control for compliantly actuated robots," *IEEE Trans. on Robotics*, vol. 34, no. 2, pp. 317–335, 2018.

[3] A. De Luca and W. Book, "Robots with flexible elements," in *Springer Handbook of Robotics*, 2nd ed., B. Siciliano and O. Khatib, Eds. Springer, 2016, pp. 243–282.

[4] J. E. Bobrow, S. Dubowsky, and J. S. Gibson, "Time-optimal control of robotic manipulators along specified paths," *Int. J. of Robotics Research*, vol. 4, no. 3, pp. 3–17, 1985.

[5] K. G. Shin and N. McKay, "Minimum-time control of robotic manipulators with geometric path constraints," *IEEE Trans. on Automatic Control*, vol. 30, no. 6, pp. 531–541, 1985.

[6] D. J. Braun, F. Petit, F. Huber, S. Haddadin, P. van der Smagt, A. Albu-Schäffer, and S. Vijayakumar, "Robots driven by compliant actuators: Optimal control under actuation constraints," *IEEE Trans. on Robotics*, vol. 29, pp. 1085–1101, 2013.

[7] N. Mansfeld and S. Haddadin, "Reaching desired states time-optimally from equilibrium and vice versa for visco-elastic joint robots with limited elastic deflection," in *Proc. IEEE/RSJ Int. Conf. on Intelligent Robots and System*, 2014, pp. 3904–3911.

[8] O. Dahl, "Path Constrained Robot Control," Ph.D. dissertation, Lund Institute of Technology, 1992.

[9] J. Kepler, *Astronomia Nova*, 1609.

[10] ——, *Epitome Astronomiae Copernicanae*, 1621.

[11] I. Newton, *Philosophiae Naturalis Principia Mathematica*, 1687.

[12] A. H. De Ruiter, C. Damaren, and J. R. Forbes, *Spacecraft Dynamics and Control: An Introduction*. John Wiley & Sons, 2012.

[13] M. Athans and P. L. Falb, *Optimal Control: An Introduction to the Theory and Its Applications*. McGraw-Hill, 2006.